

## SPECTRAL WAVE MODELLING IN TIDAL INLET SEAS: RESULTS FROM THE SBW WADDEN SEA PROJECT

Ap van Dongeren<sup>1</sup>, André van der Westhuysen<sup>2</sup>, Jacco Groeneweg<sup>3</sup>, Gerbrant van Vledder<sup>4</sup>,  
Joost Lansen<sup>5</sup>, Alfons Smale<sup>6</sup>, Caroline Gautier<sup>7</sup>, Herman Peters<sup>8</sup> and Ivo Wenneker<sup>9</sup>

Over the last five years a research program has been carried out to assess the performance of the spectral wave model SWAN in the Wadden Sea so that it may be used for the transformation of offshore wave conditions to wave boundary conditions near the sea defenses (dikes and dunes). The assessment was done on the basis of extensive wave measurements conducted in Ameland inlet and the Dutch Eastern Wadden Sea, as well as relevant data from lakes and estuaries. After a first round of assessment, we found that SWAN performed reasonably well for storm conditions but three aspects required further attention. Firstly, over the tidal flats the computed ratio of integral wave height over water depth showed an apparent upper limit using the conventional Battjes and Janssen (1978) depth-limited wave breaking formulation, because the wave growth over finite depth is hampered by the present formulation of depth-induced wave breaking. The problem has been solved using a new breaker formulation. Secondly, focusing on the main channel, SWAN formulations needed to be modified in order to eliminate overprediction of the significant wave height in opposing currents. Thirdly, the primary spectral peak of North Sea waves penetrating into the inlet was underpredicted. Best results were obtained when the refraction of low-frequency waves was limited and the bottom friction coefficient was set at a lower value than the current default for wind seas. All these improvements have lead to a wave transformation model with which reliable wave conditions in the Wadden Sea and related complex areas can be determined.

*Keywords: Wave modelling, Tidal inlets, SWAN, Wadden Sea, Spectral wave models, wave breaking dissipation, wave-current interaction.*

### INTRODUCTION

A significant part of the Netherlands lies below sea level and is protected from flooding by dunes and dikes. In compliance with the Dutch Flood Defences Act ('Waterwet, 2009'), the safety of these Dutch primary sea defences must be assessed every six years for the required level of protection. This assessment is based on the Hydraulic Boundary Conditions (HBCs) and the Safety Assessment Regulation (VTV). In order to compute these HBCs at the toe of the dikes and dunes, offshore wave statistics are transformed using the spectral wind wave model SWAN (Booij et al., 1999) which is widely used for the computation of wave fields over shelf seas, in coastal areas and in shallow lakes.

Until 2006 this procedure could only be applied for sea defences along the west coast of the Netherlands, including the uninterrupted Holland coast and the Scheldt estuaries in the southern part of the Netherlands. It was not applied in the complex Wadden Sea tidal inlet system where there were uncertainties regarding the quality of the model's performance. For instance, Kaiser and Niemeyer (2001) showed that SWAN seems to underestimate the penetration of low-frequency storm waves from the North Sea into the tidal inlet of Norderney in the German part of the Wadden Sea. In addition, up until recently no relevant wave data were available to validate and improve the SWAN model for the Dutch Wadden Sea region. Therefore, in 2002 an extensive measurement campaign was set up in the tidal inlet of Ameland (Zijderveld and Peters, 2008) to fill this data need. In 2006 an additional set of measurement devices was deployed in the eastern Wadden Sea.

In 2006, the Dutch Public Works Department (Rijkswaterstaat) awarded Deltares a commission to assess the performance of the wave transformation model SWAN as part of a larger five-year project called SBW (Strengths and Loads of Sea Defenses). In this project, Deltares (formerly Delft

---

<sup>1</sup> Deltares Delft, Netherlands, ap.vandongeren@deltares.nl

<sup>2</sup> Deltares Delft, Netherlands, andre.vdwesthuysen@deltares.nl

<sup>3</sup> Deltares Delft, Netherlands, jacco.groeneweg@deltares.nl

<sup>4</sup> Alkyon Arcadis, vledder@alkyon.nl

<sup>5</sup> Royal Haskoning, j.lansen@royalhaskoning.com

<sup>6</sup> Witteveen and Bos, a.smale@witteveenbos.nl

<sup>7</sup> Svasek (now at Deltares) Netherlands, caroline.gautier@deltares.nl

<sup>8</sup> Rijkswaterstaat – Data Dienst, herman.peters@rws.nl

<sup>9</sup> Deltares Delft, Netherlands, ivo.wenneker@deltares.nl

Hydraulics) has worked with Rijkswaterstaat's Data Division who collected data, and with researchers from universities and Dutch consultants, Alkyon Arcadis, Royal Haskoning, Svasek, Witteveen+Bos to perform hindcasts and analyze the results. This paper will discuss the method with which the project was executed and show the most important findings, which will be of interest to the broader community of wave modellers.

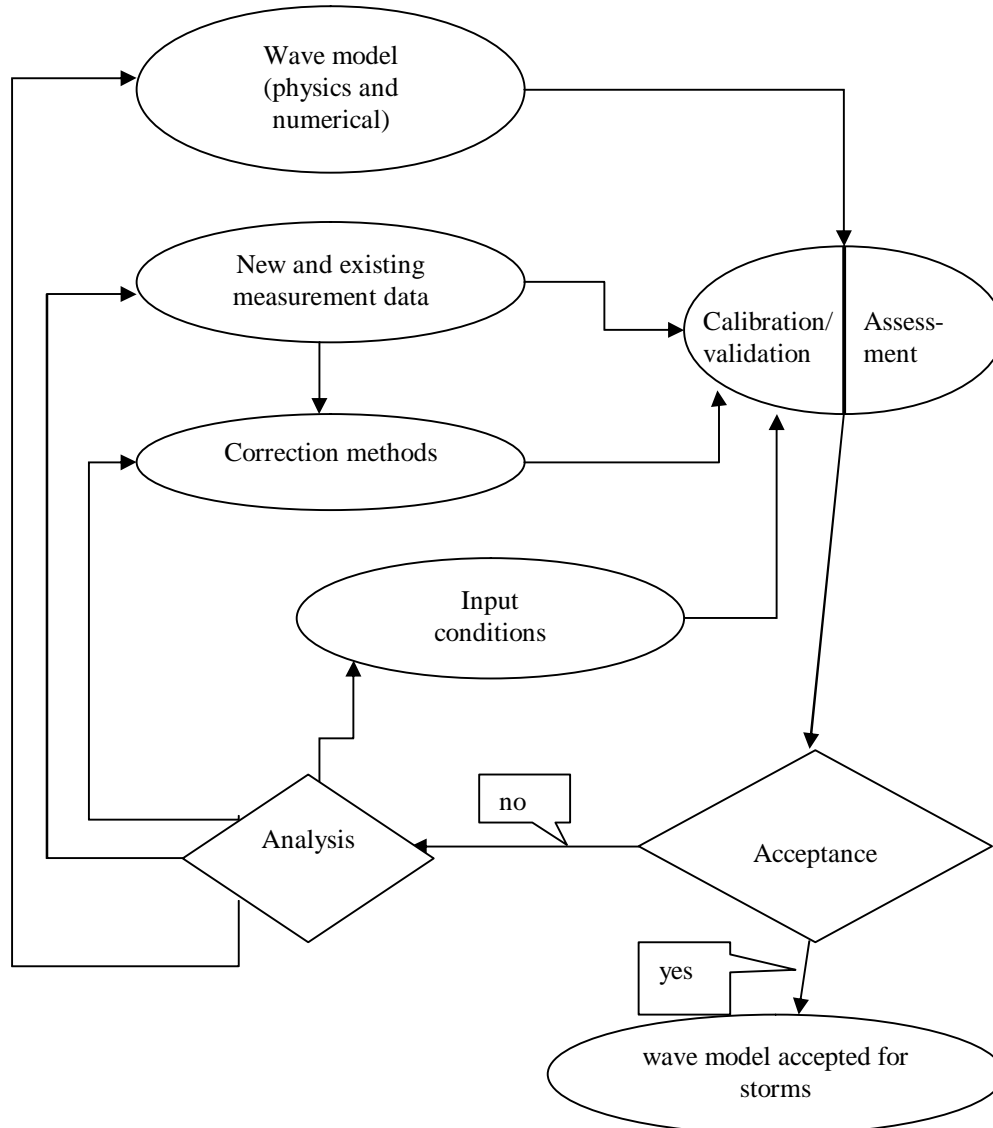


Figure 1: Schematic representation of the model improvement strategy

### MODEL IMPROVEMENT STRATEGY

The very first step in the project was an investigation into the state of the model and model results. To that end we interviewed wave model experts (researchers and consultants), stakeholders (local waterboards) and policy makers (national government). This information led to a Plan of Action which was structured around a model improvement strategy. This strategy is visualized as a cyclic process, see Figure 1 and was reported in WL|Delft Hydraulics (2006a).

The effort starts (on the top right-hand side) with an assessment of the model, made through storm hindcasts using existing measurement data and using the latest version of the model (at the start of the project SWAN 40.41AB, <http://swan.tudelft.nl>). The hypothesis was that the model results would not be accurate enough for immediate acceptance. This turned out to be true and an analysis was made to determine the origin of the greatest uncertainties in the model-data mismatch. Assuming

the measurements have been carried out with sufficient accuracy, the cause must be sought in the model itself (physics, numerical aspects) or in the computed input for the model (i.e., HIRLAM hindcasted wind fields and current- and water level fields from a Delft3D or WAQUA surge model).

In the cycle of model assessment and improvements various hypotheses will be formulated and tested. For instance, the analysis can also show that sufficiently accurate wave boundary conditions can be obtained with only limited corrections to the wave parameters that have been determined. One of the results of the analysis could also be that there is a lack of suitable measurement data and that it is necessary to carry out additional field measurements. The new measurement data is then used in a new assessment of the existing model. This provides information so as to improve model formulations and assess the quality of the input fields (wind, water level, currents and bathymetry). In the end, the aim is to produce a model which is acceptable for use in storm conditions and which can be used to compute the HBCs in the Dutch Wadden Sea. This last step is not trivial. The HBCs are computed for 1/4000 per year conditions which are far more extreme than the storms that have been measured. If we use a model which is performing well for storm conditions for HBC calculations we make the implicit assumption that the physics of the transformation process is essentially the same.

#### EFFECT OF WIND-DRIVEN CURRENTS ON WAVES AT NORDERNEY

In the first cycle of the project WL|Delft Hydraulics (2006b) confirmed that the model was underestimating the wave conditions behind Norderney island at RIFFGAT station as reported by Kaiser and Niemeyer (2001). While the wave directions were predicted accurately in the frequency range with significant energy density, the measured spectrum showed a distinctly more fully-grown shape (lower peak frequency and a larger wave height) in the measurements, see Figure 2 (black line) than the modelled spectrum does (magenta line).

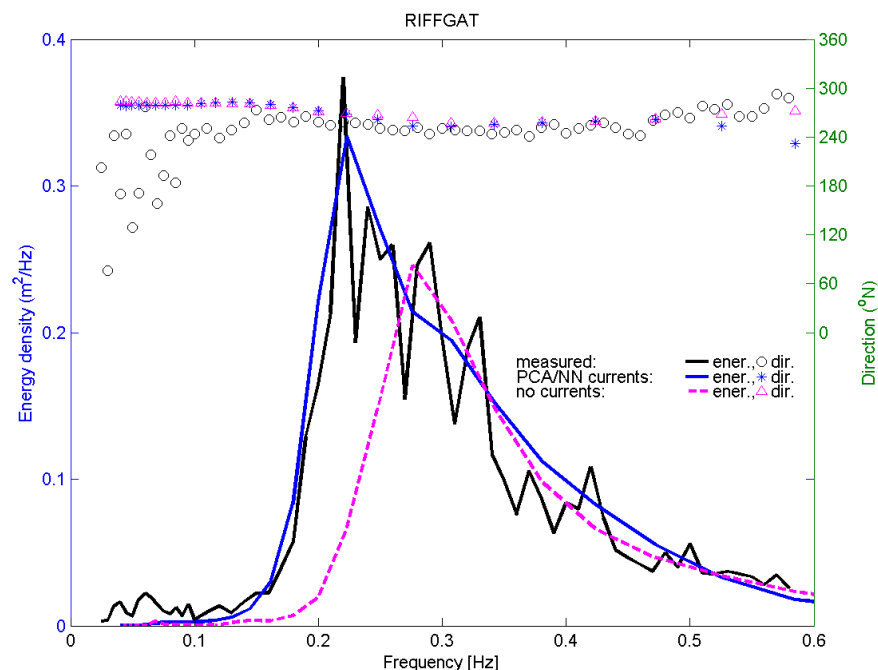


**Figure 2 Measured (black solid), modelled with current (blue solid) and modelled without current (magenta dashed) spectra at RIFFGAT**

WL|Delft Hydraulics and Alkyon (2007) found that this deficiency could be explained by including residual tidal and wind-driven currents. Since the spectra were measured at astronomical slack tide, previous investigations did not take the currents into account. However, in these storm conditions a significant wind-driven current is present. The modelled current field (Herman et al.,

2006) (not shown) reveals that currents run across the inlet from southwest to northeast and turn just south and west of Norderney island in a counterclockwise fashion, where they have a more northerly and westerly direction and “jet” out of the inlet. Applying this current field causes the local waves (driven by winds from the northwest) to experience a mostly opposing current before they reach RIFFGAT, decreasing their effective wave age and thus increasing the growth in the wave height and mean wave period (visible as the larger area and the smaller peak frequency of the blue spectrum). The result (blue line in Figure 2) agrees well with the measured spectrum for this storm. This finding resolved one of the a priori issues which cast doubt on the applicability of the SWAN model in tidal inlet seas and stressed the need to include currents in tidal inlet sea computations.

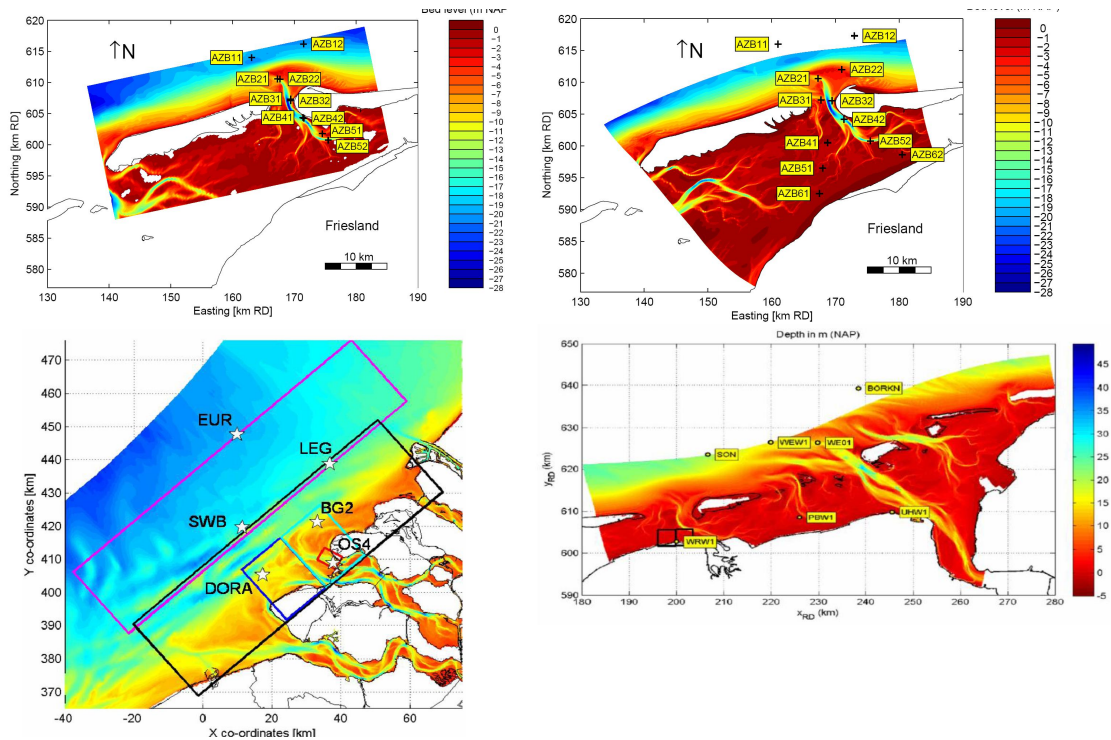


**Figure 3: Wave buoy locations. Top left: Amelander Zeegat storm season 2005-2006. Top right: same, storm season 2006-2007. Bottom left: Eastern Scheldt. Bottom right: Eastern Wadden Sea.**

### ASSESSMENT OF MODEL PERFORMANCE IN THE AMELANDER ZEEGAT

While it is reasonable to assume that the German Wadden Sea is subject to the same dominant physical processes as the Dutch part, the next issue in the first cycle was to assess the performance in the Dutch Wadden Sea itself. Based on then available measurements in the Amelander Zeegat in The Netherlands (for layouts see Figure 3 top left), we found that the model performance was not unreasonable, especially after including current fields. However we did find a number of issues that demanded further attention:

Firstly, from finite-depth wave growth situations in lakes, it is known that wave heights are underestimated in SWAN (De Waal et al., 1997). The expectation was that this model deficiency is relevant for the computation of wave boundary conditions in the Wadden Sea since most sea defenses are adjacent to extensive tidal flat areas. After a re-deployment of the wave buoys before the 2006-2007 storm season (Figure 3, top right), we verified whether this phenomenon occurred in the Wadden Sea.

Secondly, the wave heights in the inlet throat were generally too high in opposing tidal currents, which confirmed similar findings by Ris and Holthuijsen (1996). This issue is addressed briefly below and extensively in Van der Westhuysen (2010b, this volume).

The third finding was that in the Amelander Zeegat measurements show that very little North Sea-generated wave energy penetrates into the inlet under storm conditions. The ebb tidal delta functions as an efficient wave dissipator and waves which do penetrate through the inlet gorge are quickly refracted out of the channels and dissipated over the flats. However, for more exposed inlets, e.g. in the Eems-Dollard estuary (situated on the Dutch-German border), significant wave penetration can be expected (and has been visually observed), already under frequently-occurring storm conditions. In order to verify the performance of SWAN with respect to wave penetration we also measured waves in the more exposed Eastern Wadden Sea near the Eems estuary (Figure 3 bottom right; note that the Borkum station has only been active since December 2007 and is not used in this paper) and used existing data from the Eastern Scheldt estuary in the southwest of the Netherlands (Figure 3 bottom left) in the second phase of the model improvement cycle.

In the remainder of the paper we will demonstrate the model improvements made with respect to finite-depth wave growth, wave-current interaction and wave penetration in the second cycle of the project.

### FINITE-DEPTH WAVE GROWTH

Data analyses (Deltares, 2008) showed that observed  $H_{m0}/d$  ratios in the Wadden Sea flat areas reach values up to 0.43. These  $H_{m0}/d$  ratios are consistent with observed data from lakes with a horizontal bathymetry (Lake IJssel and Lake Sloten in the Netherlands and Lake George, Australia), see Figure 4 (left). Here, the  $H_{m0}/d$  ratios are a function of the non-dimensional depth, defined as  $gd/U_{10}^2$ . Lake Sloten and Lake IJssel can be identified as two distinct populations while the Amelander Zeegat and Lake George data cover both other populations. This last point is an important finding since it allows lake data to be used for the assessment of the wave model for the finite-depth wave growth aspect in the Wadden Sea (and vice versa). The reason for the two distinct populations for Lake IJssel and Lake Sloten is unknown at this point but the hypothesis is that it has a relation with ripple heights in either lake (Deltares, 2008) which does not enter the scaling.

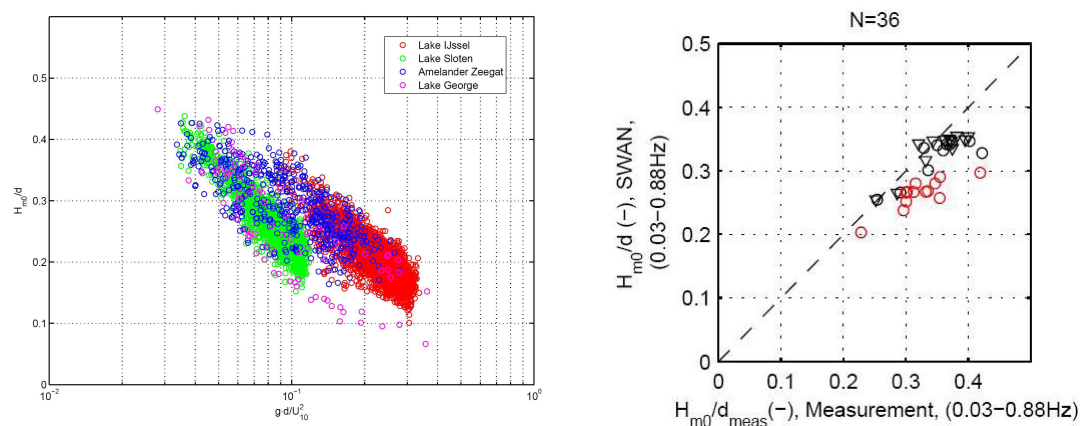


**Figure 4: Left: non-dimensional wave height versus  $U_{10}$  scaled depth. Right: scatter plot of  $H_{m0}/d$  model improvement. black triangle: AZB51. Black circle AZB61, red circle AZB62.**

Model validation studies of finite-depth growth using stationary cases for storms of the 2006-2007 season and the 2007-2008 season (Royal Haskoning, 2008 and Witteveen+Bos, 2008 respectively), showed quite similar results, even though the storms were different. Here we will show results by Royal Haskoning (2008). The scatter plot (Figure 4 right) shows that the predicted wave height over depth ratio underestimates the observations for high values of  $H_{m0}/d$ . The model result ratio does not exceed 0.38, whereas the observed ratio is about 0.43.

For all situations (which were run in stationary mode) and at all three wave buoy locations the computed wave energy spectra show less wave growth compared to the measured spectra (not shown here), and thus less wave height. It appears that the wave growth over nearly horizontal regions is hampered by the present default surf breaking mechanism in SWAN, the Battjes-Janssen (1978) model with  $\gamma=0.73$ , leading to underprediction of the significant wave height  $H_{m0}$  and spectral wave

period  $T_{m-1,0}$ . This is an indication that this formulation of depth-induced breaking obstructs the wave growth over horizontal bathymetries too strongly. The finding is consistent with earlier findings for Lake IJssel (De Waal et al., 1997; using SWAN's predecessor HISWA) and for Lake Sloten (Alkyon, 2003). In order to improve the agreement with the observations, either the value of the  $\alpha$  parameter had to be decreased or the value of the  $\gamma$  parameter had to be increased (the latter to a value of about 0.8-0.9). However, the tuning of either parameter is equivalent (Dingemans, 1998 p. 324) and therefore  $\alpha$  can be held fixed at unity and  $\gamma$  can be varied.

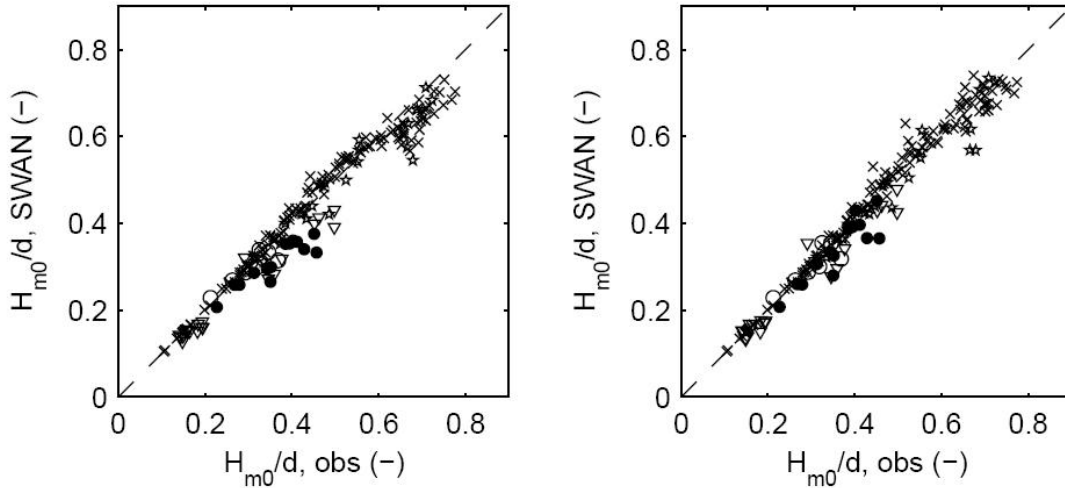


**Figure 5: Scatter plots of model results versus observations of the validation subset for the BJ78 model (with BJ = 0.73, left-hand panels) and with the biphasic model (9). Plotted are results of Amelander Zeegat interior buoys (filled circles), Lake IJssel (open circles), BJ78 data set (stars), Smith (2004) (crosses) and Amelander Zeegat ebb tidal shoal buoys (inverted triangles). Figure reproduced from Van der Westhuijsen (2009).**

Van der Westhuysen (2009, 2010a) found that the optimal value of  $\gamma$  (based on minimizing the bias and scatter index) is different for different data sets, where clearly two populations can be discerned: one for beaches and one for finite-depth wave growth cases. For both wave height and wave period, the beach cases show a minimum for  $\gamma$  values around 0.6-0.8, i.e. around the commonly-used default of  $\gamma=0.73$ , whereas for the nearly-horizontal bed cases the errors are monotonically decreasing with increasing  $\gamma$ . This points to a fundamentally different physics, where depth-limited wave breaking should be effectively absent in the case of finite-depth wave growth over horizontal bottoms.

Van der Westhuysen (2010a) proposed to modify the breaker formulation by Thornton and Guza (1983) which itself is a modification of Battjes and Janssen (1978) to solve the underestimation of wave height in such conditions. Van der Westhuysen (2010a) shows that the fraction of breaking waves in this expression can be expressed as a power law of the biphasic of the wave field. The biphasic is a measure of the nonlinearity of the waves as they propagate from deeper water (when they are approximately sinusoidal) to intermediate depth (when they become more “peaked” or skewed) and into shallow water when they have a sawtooth shape and they become asymmetric. Because SWAN is not a nonlinear wave-by-wave model, it can not compute the biphasic of the waves. However, Doering and Bowen (1995) and Eldeberky (1996) related the biphasic to the Ursell number which can be computed by SWAN. Figure 5 (from Van der Westhuijsen 2010b) shows that the bias and scatter index decrease (slightly and substantially, respectively) and – more importantly – that the apparent upper limit in the modelled  $H_{m0}/d$  values for the Amelander Zeegat (black circles) disappears when the biphasic model of Van der Westhuysen (2010a) is applied (see van der Westhuijsen (2009) for details) Also for the cases with beach profiles the bias in  $H_{m0}/d$  values decreases.

## WAVE-CURRENT INTERACTION

As mentioned before, observations in the tidal channel are typically well reproduced in following currents, but under strong opposing currents, wave heights are significantly overestimated. Ris and Holthuijsen (1996) propose that such overestimations are due to insufficient steepness dissipation of

waves on opposing current. Van der Westhuysen (2010b, this volume) presents a new formulation for the enhanced dissipation of waves on a counter current which is scaled with the local spectral saturation (steepness) and the degree of Doppler shifting per spectral component. This formulation is suitable for both mature wave fields and young wind sea conditions. This expression contains one additional unknown parameter, which was calibrated using laboratory and field observations. Validation of this enhanced dissipation term for field cases of the Ameland Zeegat shows an improvement for opposing current situations in the tidal channel. For situations with following current, no significant deterioration in results is found. In particular, the results for the young wind sea on the tidal flats are not significantly affected, unlike with the expression of Ris and Holthuijsen (1996). However, since the remaining dissipation terms in SWAN have been calibrated without this enhanced dissipation term, the addition of the proposed formulation results in some deterioration of the overall statistics.

### **PENETRATION OF NORTH SEA WAVES**

The performance of SWAN with respect to wave penetration was assessed using field cases of the Eastern Scheldt estuary in the southwest of the Netherlands, and the Dutch Eastern Wadden Sea. Svasek (2007) investigated the penetration of North Sea waves into the mouth of the Eastern Scheldt for a number of storms which had a pronounced offshore peak, and for which buoy measurements and a recent bathymetric survey were available. The bathymetry and location of the buoys are shown in Figure 3 (bottom left). Run in stationary mode, the results all show that the North Sea wave spectral peak (around 0.12 Hz) is properly modelled for the first three stations (first three rows in Figure 6) but not for the innermost station OS4 (last row). Note however that the vertical scale (i.e. the energy density) has decreased significantly. The main mismatch is that the modelled swell energy peak is much lower than the measurements in station OS4.

Svasek (2007) found that decreasing the bottom friction increased the inshore energy over the swell frequency range a little. Alkyon (2008a) further analysed the reduction of the North Sea wave spectral peak by investigating the spectra in detail and found that the rapid change in the spectral shape did not occur when any source or sink terms (breaking, whitecapping, etc.) were locally large. By elimination, this suggests that the cause of the mismatch is in the propagation terms and or small-magnitude, but persistent, sink terms such as the bottom friction that act over large distances.

This was investigated further using observations in the Eastern Wadden Sea (Figure 3, bottom right). Alkyon (2008b) investigated the wave transformation for the storm of 8-9 November 2007 and found that as in the Eastern Scheldt, the low-frequency components were underpredicted at the location of the most shoreward buoys, see Figure 7. At the outer buoy WEO1 the model-data agreement is reasonable (even though the peak is somewhat underestimated) but in all the inner buoys there is a significant amount of energy below 0.2 Hz that the model does not predict. Note the change of scale from the outer to the inner buoys. The high-frequency flank of the spectrum is predicted very well. We verified that the low-frequency variance is not explained by lower-harmonic bound waves (Hasselmann, 1962 Herbers et al., 1995) which are not computed by SWAN.

Spatial plots of the low-frequency wave height  $H_{10}$  (which is defined as the significant wave height computed over the frequency interval from 0 to 0.1 Hz) and low-frequency mean wave direction, see Figure 8, show that the modelled incoming low frequency waves come from NNW over the North Sea. In the channel area just north of PBW1, the waves change direction, presumably due to refraction over the flats into the channel and back. The effect of this refraction is that the modelled low-frequency energy does not reach the station PBW1. The  $H_{10}/H_{m0}$  ratio is about 0.10 there whereas it should be about 0.3. It is clear that the wave energy does not penetrate far enough towards the shore due to propagation and bottom friction dissipation effects.

Analyzing the propagation effects, Deltares/Alkyon (2009) compared results from the spectral wave model SWAN and the mild-slope model PHAROS that includes diffraction. They found that refraction was dominant with diffraction being local and having a negligible effect on the amount of energy that penetrates. This finding eliminates an uncertainty in SWAN with respect to the need to include diffraction for the purpose of computing HBC in the Wadden Sea, but does not give an

explanation for the reported underestimation of the low frequency components. This leaves a reduction of the bottom friction coefficient (using a uniform value of  $C_{f,JON}=0.038 \text{ m}^2\text{s}^{-3}$ , as opposed to the usual setting of  $C_{f,JON}=0.067 \text{ m}^2\text{s}^{-3}$ , as recommended by Bouws and Komen (1983) for fully – developed wind seas) as a possible solution to the underestimation. In addition, to account for the remaining uncertainties in the propagation, the refraction of low-frequency components was limited in the model. These two so-called fall back options were used to tune the model such that it produces low frequency wave heights at the sea defenses which correspond to measured values (Deltares, 2009).

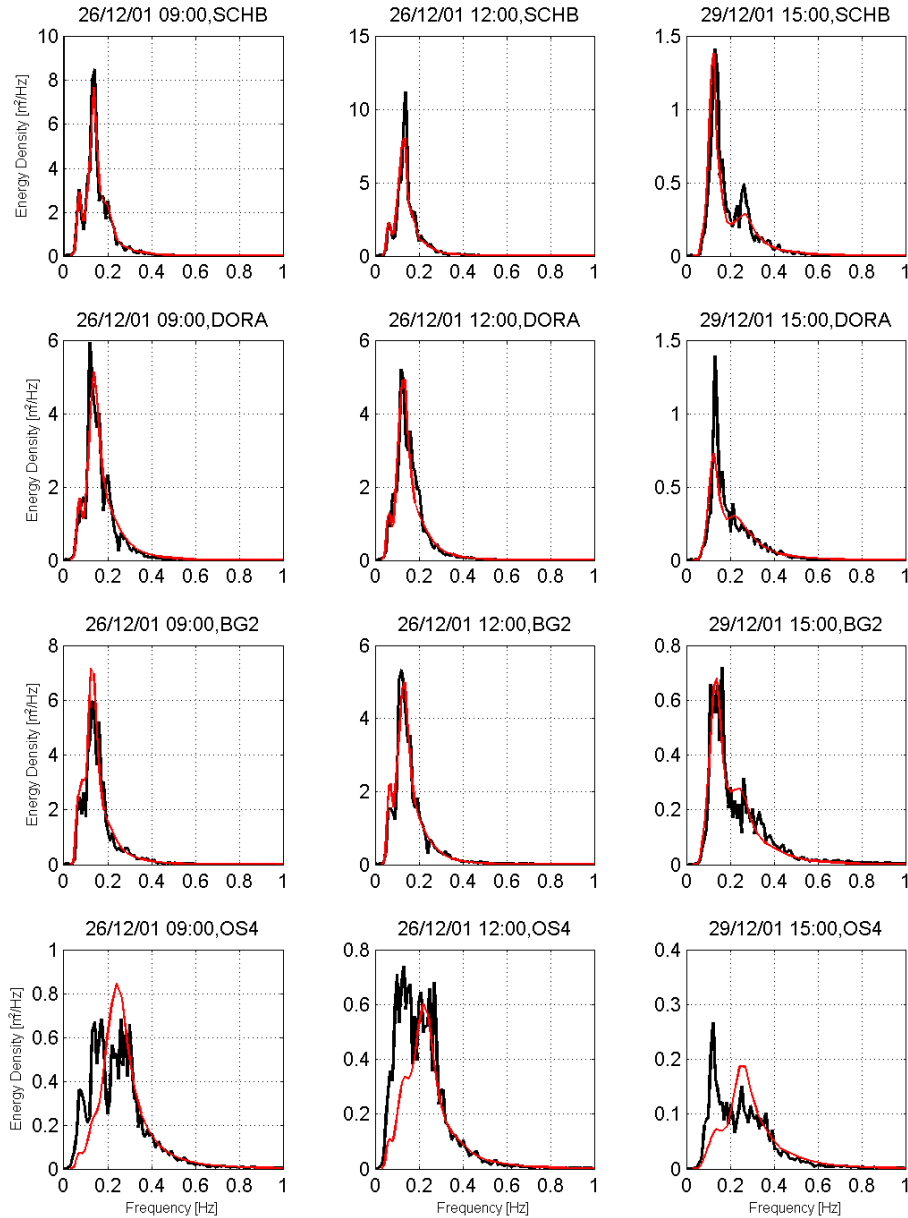


**Figure 6: Measured (black) and modelled (red) spectra at three different instants of a storm (columns) for four different stations (rows) in the mouth of the Eastern Scheldt.**

In order to reduce the influence of refraction on the propagation of the low-frequency wave components, the spectral velocity term  $c_0$  of the action balance equation is multiplied with a frequency dependent limiter  $F_0$  (ranging from 0 to 1)

$$F_{\theta} = \begin{cases} (f / 0.2)^2 & f \leq 0.2 \text{ Hz} \\ 1 & f > 0.2 \text{ Hz} \end{cases} \quad (1)$$

where  $f$  is the frequency in Hz. In the remainder we will show the results at the peak water level during the storm of 9 November 2007, which is the only measured storm in the area. The effect of limiting the refraction (Figure 9 left) is to enhance the low-frequency peak at a frequency of about 0.08 Hz for both nearshore buoys UHW1 and WRW1. This is because low-frequency energy does not refract out of the channels as much as in the default and now reaches the sea defenses. The modelled values (red) are fairly close to the measurements (black) but there is still a mismatch. Figure 9 (right) presents the variation along the transect near the coast of Friesland and Groningen (Figure 3, bottom right). The location of the WRW1 and UHW1 buoys along this transect are indicated with a vertical bar, and their measured values are shown by a black circle. The significant wave height  $H_{m0}$  shows only a slight increase relative to the default case, and matches the measured values almost perfectly for both buoys (within 10%). The spectral mismatch reveals itself in the spectral period  $T_{m-1,0}$  which is consistently underpredicted relative to the measurements (by about 15%). The fallback option increases the value of the parameter near the locations of the buoys by about 20% relative to the default. There is no increase in the middle part of the transect due to the fallback option ( $x=210 - 220$  km) which is a flat area well away from the tidal channels, and therefore not sensitive to refraction. The values of low-frequency parameters  $H_{20}$  and  $T_{20}$  (which is computed as the spectral period  $T_{m-1,0}$ , but now only over the frequency range 0 - 0.2 Hz) increase by about 0.1 m and 1.7 s, respectively, a percentual increase of about 20-50% for the wave height and about 30% for the wave period along the transect. The measured  $T_{20}$  period is now almost perfectly matched at the buoys, whereas the fallback option bridges about one-third of the gap between the default computation and the measured value of the low-frequency wave height.

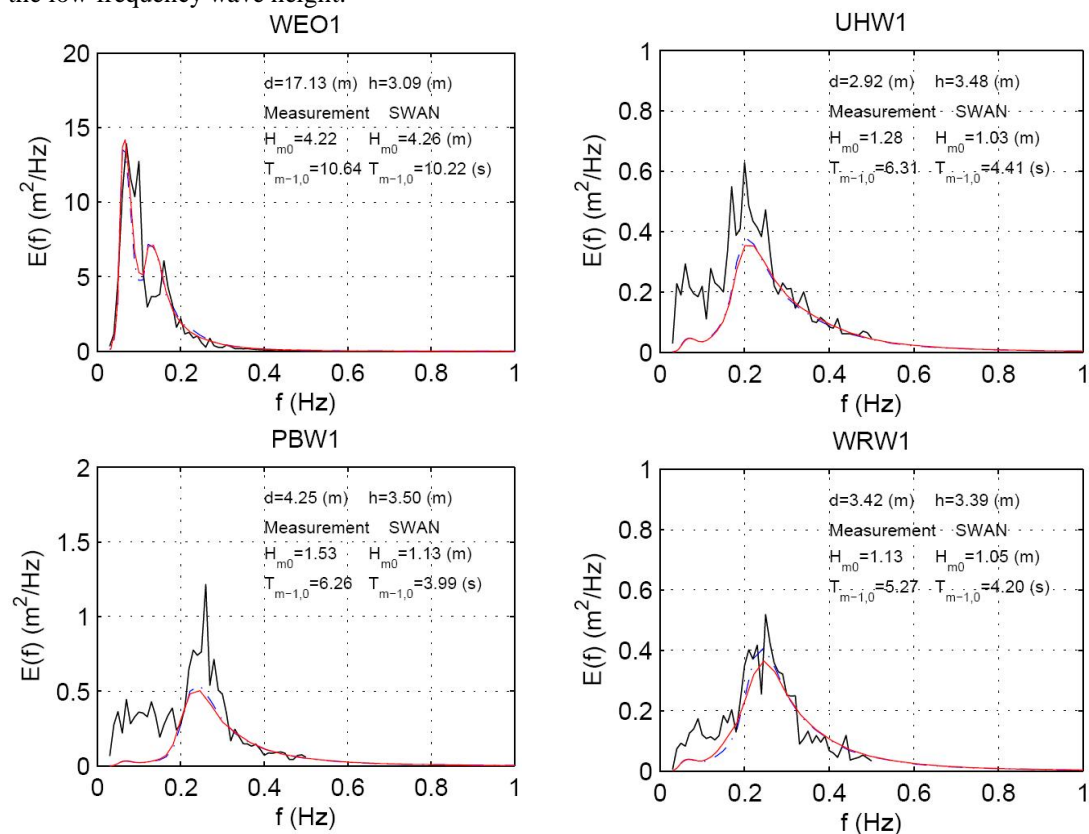


Figure 7: Measured (black), modelled (red) and modelled without currents (blue dashed) spectra at four stations for the storm of 8-9 November.

When only the bottom friction is reduced, the low-frequency flank of the spectra at UHW1 and WRW1 (which are located near the sea defenses) is increased, relative to the default, but falls still short of the measurements (Fig. 10 left). The variation of the wave parameters along the transect near the sea defenses (Fig. 10 right) show a spatially-uniform increase in the  $H_{m0}$  wave heights and  $T_{m-1,0}$  wave period (red lines, relative to the default black lines). This increase is more uniform than for the previous fallback option. The predictions are within 10% of the measured values for the significant wave height, and within 20% for  $T_{m-1,0}$ . The low-frequency wave height  $H_{20}$  and wave period  $T_{20}$  also increase almost uniformly, resulting in a good match with data at WRW1 and an underprediction of about 25% for both low-frequency wave height and period at UHW1. These results confirm the concurrent findings of Zijlema (2009).

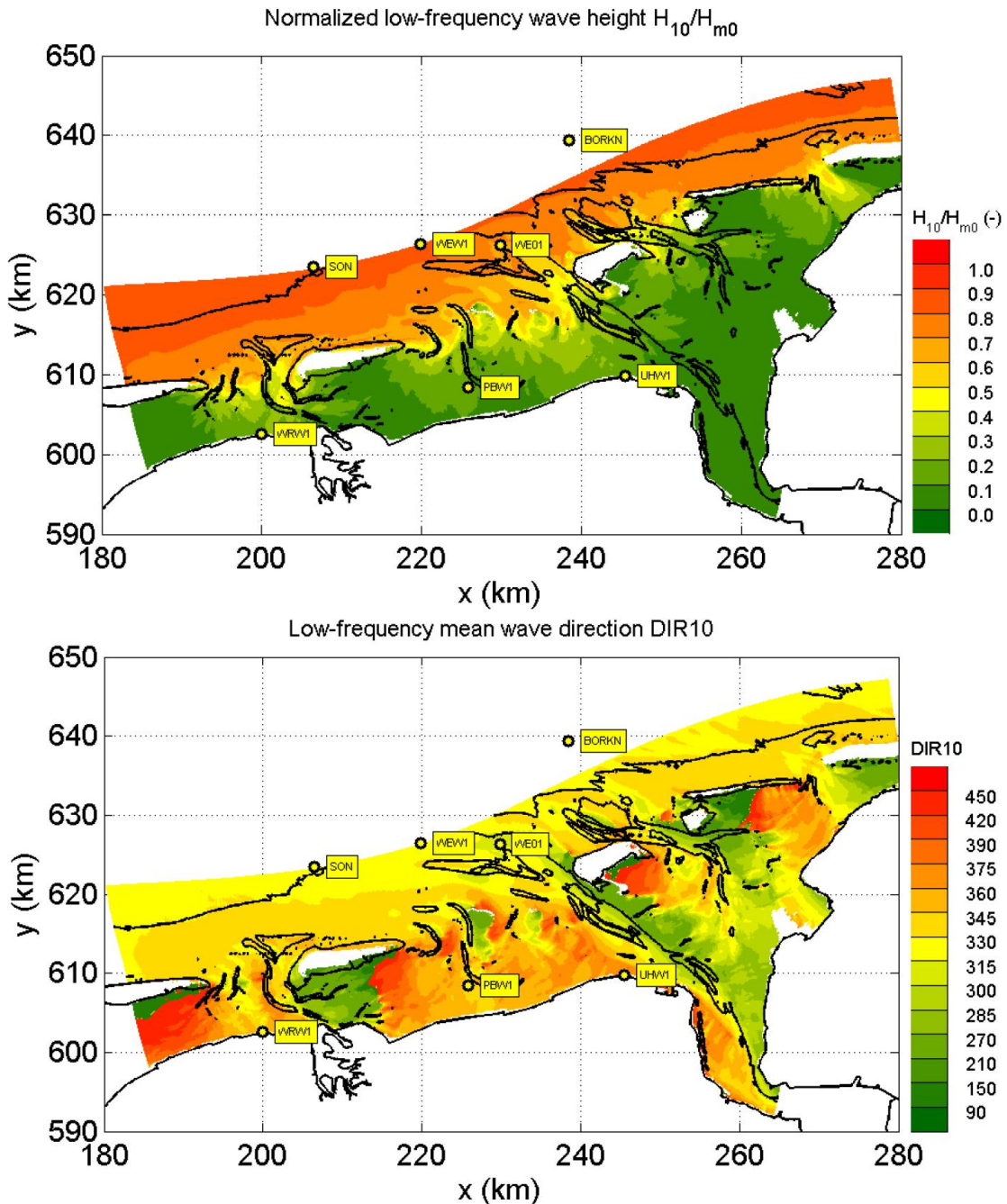
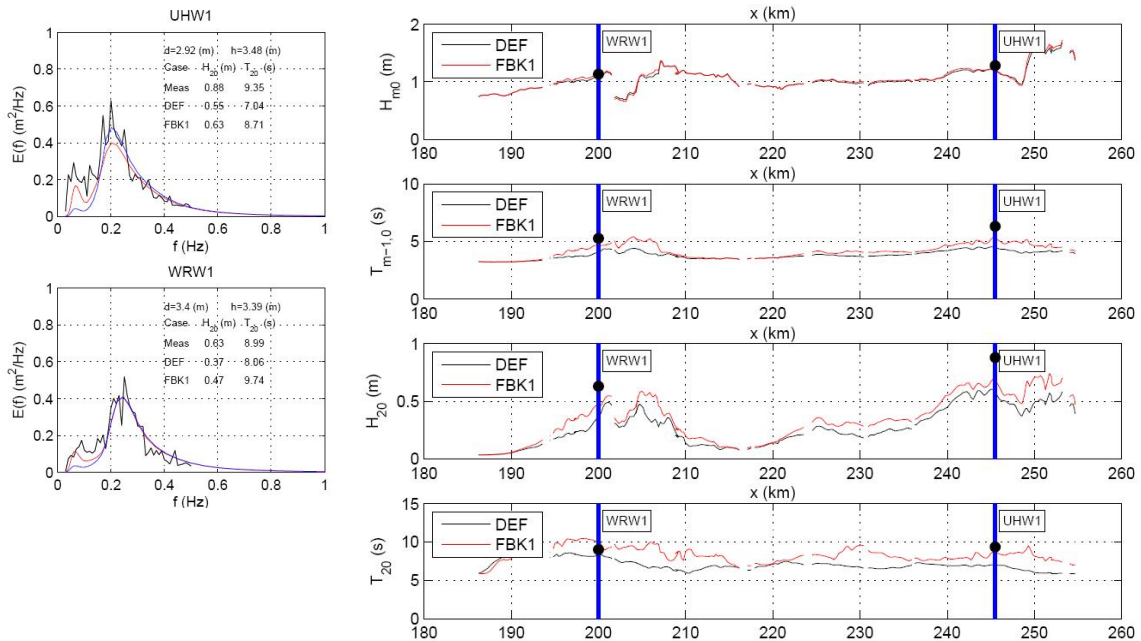


Figure 8: Normalized low frequency wave height (top) and mean low-frequency wave direction (bottom) in the Eastern Wadden Sea.

The best results are obtained when the two options are applied together (Figure 11). The spectral density in the low-frequency range ( $f < 0.2$  Hz) is increased due to the reduced bottom friction and limited refraction and agrees rather well with the data. The transect plots (Figure 11 right panel) show that the increase in significant wave height  $H_{m0}$  is dominated by the reduced friction, whereas the increase in  $T_{m-1,0}$  is due to an almost equal contribution of the two model options. The significant wave heights and mean energy wave periods ( $T_{m-1,0}$  and  $T_{20}$ ) at WRW1 and UHW1 are well predicted (within 10%). The increase in  $H_{20}$  is also due to the combination of the two effects with a dominance of the friction component in the western and central section of the transect. Limiting refraction has the largest effect at the eastern end (around UHW1) and in specific locations such as at  $x=205$  m (at the end of the Zoutkamperlaag channel). The increase in  $T_{20}$  is largely dominated by the limiter on refraction with the reduced friction increasing overall levels. The low-frequency wave heights and periods at WRW1 and UHW1 are now well predicted for the case of high water.



**Figure 9: Left: Measured (black), default (blue) and limited refraction (red) spectra for two locations on the sea defense. Right: Default (black), limited refraction (red) results for total significant wave height, mean energy period, low-frequency wave height and low-frequency period along a transect along the coastline. Measured values are indicated with black solid circles on the vertical blue lines.**

In terms of statistics, the regression coefficients of modelled vs. observed values of the  $H_{20}$  parameter improves from a value of  $c = 0.44$  (default) to 0.54 (limited refraction), 0.56 (lower bottom friction coefficient) and 0.68 (combination) (where  $c=1$  would be ideal). The  $c$ -values improve to unity for the low-frequency wave period.

While limiting the refraction improves the results in the Eastern Wadden Sea, the measure is not based on physical reasoning (rather it is in defiance of it). This means that it may not be generally applicable to other water systems. On the other hand, the effect of limiting refraction may reduce if the high water levels associated with the norm events (much higher than storm levels) are applied. With respect to the reduced bottom friction, in the present formulation the bottom friction coefficient is a free parameter for which two default values are given by Booij et al. (1999). The first of these values was derived for swell conditions observed during the JONSWAP experiment (Hasselmann et al. 1973) which yielded a value  $Cf_{JON} = 0.038 \text{ m}^2 \text{ s}^{-3}$ . For fully-developed wind-sea conditions in shallow water a second value of  $Cf_{JON} = 0.067 \text{ m}^2 \text{ s}^{-3}$  was found by Bouws and Komen (1983). However, close inspection of their paper reveals some inconsistencies in the determination of the friction coefficient for wind seas (Van Vledder et al., 2010). For the present purpose which concerns the penetration of low-frequency wind waves the “swell” value of  $Cf_{JON} = 0.038 \text{ m}^2 \text{ s}^{-3}$  seems justified and gives the best results. Deltares (2009) has shown that the bottom friction coefficient if calculated

using the Madsen et al. (1988) formulation is a function of the observed sand grain diameter. The resulting bottom friction coefficient using field data corresponds more closely to the higher default value at the buoy locations but has a value around  $Cf_{JON} = 0.038 \text{ m}^2 \text{ s}^{-3}$  close to the mainland coast. We are therefore confident that application of the lower value for bottom friction is justified.

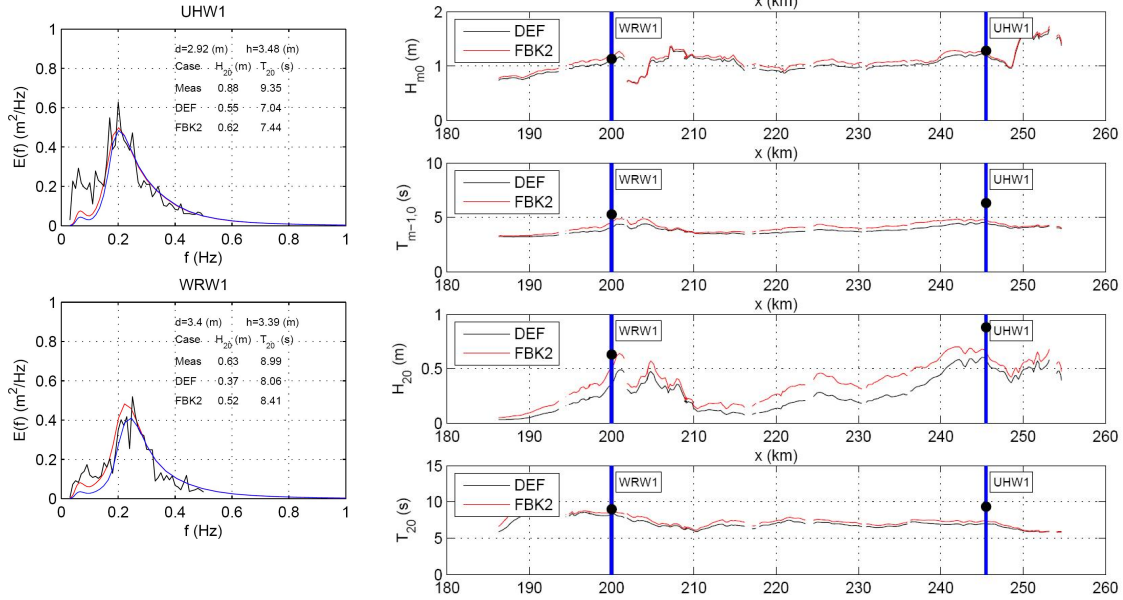


Figure 10: Left: Measured (black), default (blue) and reduced bottom friction (red) spectra for two locations on the sea defense. Right: Default (black), reduced bottom friction (red) results for total significant wave height, mean energy period, low-frequency wave height and low-frequency period along a transect along the coastline. Measured values are indicated with black solid circles on the vertical blue lines.

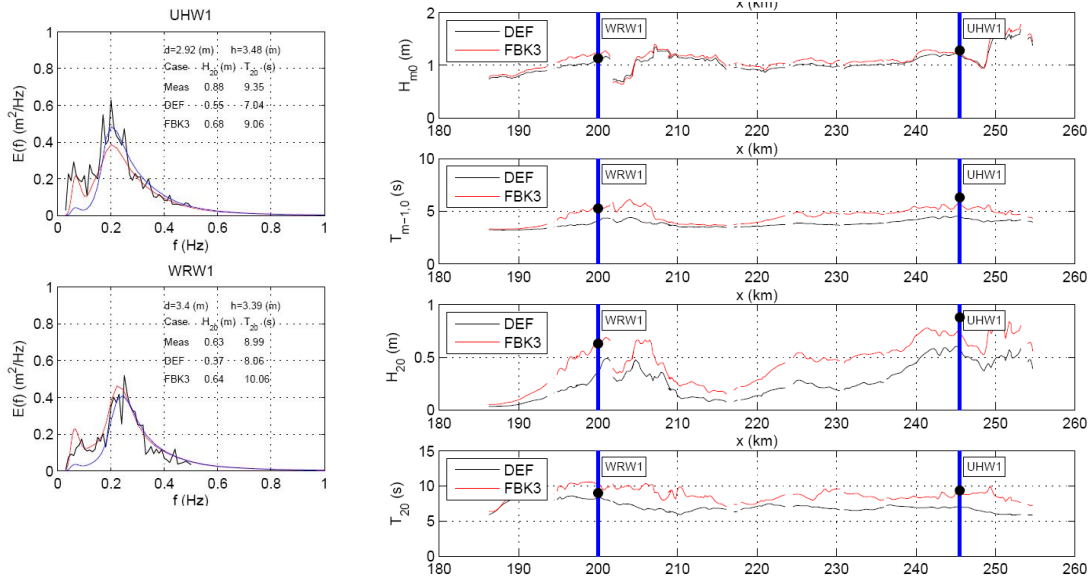


Figure 11: Left: Measured (black), default (blue) and limit on refraction and reduced bottom friction (red) spectra for two locations on the sea defense. Right: Default (black), limit on refraction and reduced bottom friction (red) results for total significant wave height, mean energy period, low-frequency wave height and low-frequency period along a transect along the coastline. Measured values are indicated with black solid circles on the vertical blue lines.

## CONCLUSIONS

Over the last five years a research program has been carried out to assess the performance of the spectral wave model SWAN in the Wadden Sea so that it may be used for the reliable transformation of offshore wave conditions to wave boundary conditions near the sea defenses (dikes and dunes). The assessment was done on the basis of extensive wave measurements conducted in Ameland the inlet and the Dutch Eastern Wadden Sea, as well as relevant data from lakes and estuaries.

We found that SWAN (SWAN 40.41AB in its default form of 2006) performed reasonably well for storm conditions but three aspects required further attention:

1. Over the tidal flats, the computed ratio of significant wave height over water depth showed an apparent upper limit using the default version of SWAN, because the wave growth over finite depth is hampered by the present formulation of depth-induced wave breaking. The problem has been solved using a new breaker formulation (Van der Westhuysen, 2010a).
2. Focusing on the main channel, a dissipation term had to be added in order to eliminate overprediction of the significant wave height in opposing currents. This has largely been achieved with a formulation for enhanced dissipation that is scaled with the degree of Doppler-induced steepening of the waves.
3. The primary spectral peak of North Sea waves penetrating into the inlet was underpredicted due to a combination of refraction and bottom friction. Best results were obtained when the refraction term was limited and the bottom friction coefficient was set at the lower value of the current two defaults (viz., the one for swell).

All these improvements have led to a wave transformation model with which reliable wave conditions in the Wadden Sea and related complex areas can be determined.

## ACKNOWLEDGMENTS

This study is part of the SBW (Strength and Loads on Water Defenses) project commissioned by Rijkswaterstaat Centre for Water Management in the Netherlands.

## REFERENCES

- Alkyon (2003). Calibration of SWAN 40.20 for field cases Petten, Sloterneer, and Westerschelde. Report A1168, Author: G.Ph. van Vledder.
- Alkyon (2008a). Analysis of SWAN hindcasts Wadden Sea, Oosterschelde Sloterneer; Investigation into low frequency wave energy, current effects and depth limitation. Alkyon Report A2085. Author: G.Ph. van Vledder.
- Alkyon (2008b). SWAN hindcast in the Eastern Wadden Sea and Eems-Dollard estuary during the Storm of 9 November 2007. Alkyon Report A2191. Authors: J. Adema, G.Ph. van Vledder and O.R. Koop.
- Battjes, J.A., and J.P.F.M. Janssen (1978). Energy loss and set-up due to breaking of random waves, *Proceedings of 14<sup>th</sup> International Conference on Coastal Engineering*, ASCE, 466-480.
- Booij, N., R.C. Ris and L.H. Holthuijsen (1999). A third generation wave model for coastal regions, Part I, Model description and validation. *J. Geophys. Res.*, 104, C4, 7649-7666.
- Bouws, E. and G. J. Komen (1983). On the balance between growth and dissipation in an extreme, depth-limited wind-sea in the southern North Sea. *J. Phys. Oceanogr.*, Vol. 13, 9, 1653-1658.
- Deltares (2008). Observed finite-depth wave growth limit in the Wadden Sea. Deltares report H5107.35. Authors: A.J. van der Westhuysen and J.P. de Waal.
- Deltares (2009). Penetration of North Sea waves into the Wadden Sea - phase 3: fallback options. Deltares report report 1200114-002. Authors: A.R. van Dongeren, A.J. van der Westhuysen, G.Ph. van Vledder and I. Wenneker.
- Deltares/Alkyon (2009). Wave propagation through tidal inlet systems. Deltares and Alkyon report 1200114-002-HYE-0006. Authors: A.J. van der Westhuysen, B. Huisman, F. Enet. O. Koop and G.Ph. van Vledder.

- De Waal, J.P., D. Beyer, J.H. Andorka Gal, L.H. Holthuijsen, G.Ph. van Vledder, J.P.F.M. Janssen and D.P. Hurdle (1997). Instelling golfmodel HISWA. Toe te passen bij productiesommen in het IJsselmeergebied. RIZA report R0269.
- Dingemans, M.W. (1998). Water wave propagating over uneven bottoms. Part 1: Linear wave propagation. *Advanced Series on Ocean Engineering*, Vol 13. World Scientific, Singapore.
- Doering, J.C. and A.J. Bowen (1995). Parametrization of orbital velocity asymmetries of shoaling and breaking waves using bispectral analysis, *Coastal Engineering*, vol. 26, no. 1-2, pp. 15-33.
- Eldeberky, Y. (1996). Nonlinear transformation of wave spectra in the nearshore zone. Ph.D. thesis, TU Delft, 203 p.
- Hasselmann, K., On the non-linear energy transfer in a gravity-wave spectrum: I. General theory, *J. Fluid Mech*, 12, 481– 500, 1962.
- Hasselmann, K., T. P. Barnett, E. Bouws, H. Carlson, D. E. Cartwright, K. Enke, J. A. Ewing, H. Gienapp, D. E. Hasselmann, P. Kruseman, A. Meerburg, O. Müller, D. J. Olbers, K. Richter, W. Sell, and H. Walden (1973). Measurement of windwave growth and swell decay during the Joint North Sea Wave Project (JONSWAP). *Dtsch. Hydrogr. Z. Suppl.* 12(A8).
- Herbers, T. H. C., S. Elgar, and R. T. Guza, Infragravity-frequency (0.005–0.05 Hz) motions on the shelf: I. Forced waves, *J. Phys. Oceanogr*, 24, 917– 927, 1994.
- Herman, A., R. Kaiser and H.D. Niemeyer (2006). Medium-term wave and current modelling for a mesotidal Wadden Sea coast. *Proc. ICCE 2006*, San Diego, pp. 628-639.
- Kaiser, R. en H.D. Niemeyer (2001). Analysis of directional spectra in shallow environment. *Proc. of 4th international symposium WAVES 2001*, 944-952.
- Madsen, O.S., Y.-K. Poon and H.C. Graber (1988). Spectral wave attenuation by bottom friction: Theory. *Proc. 21st Int. Conf. on Coastal Eng., ASCE*, pp. 492-504.
- Ris, R.C. and L.H. Holthuijsen. 1996. Spectral modelling of current wave-blocking. *Proceedings of 25th International Conference on Coastal Engineering*, ASCE, 1247-1254.
- Royal Haskoning (2008). Hindcast Ameland Zeegat storms January and March 2007 (revised). Royal Haskoning Report 9T5842.A0/R0004, October 2008. Authors: Joost Lanssen, Sjaak Jacobse, Maarten Kluyver, Erik Arnold.
- Smith, J. M. (2004). Shallow-water spectral shapes. *Proc. 29th Int. Conf. Coastal Eng., ASCE*, 206– 217.
- Svasek (2007). Hindcast tidal inlet Eastern Scheldt, Storms December 2001 and December 2003, Svasek Report CG/1461/07542/A, December 2007 Authors: C. Gaultier and M. van de Boomgaard.
- Thornton, E.B. and R.T. Guza (1983). Transformation of wave height distribution, *Journal of Geophysical Research*, vol. 88, no. C10, pp. 5925-5938.
- Van der Westhuysen, A.J. (2009). Modelling of depth-induced wave breaking over sloping and horizontal beds. *Proc. 11th International Workshop on Wave Hindcasting and Forecasting*.
- Van der Westhuysen, A.J. (2010a). Modelling of depth-induced wave breaking under finite-depth wave growth conditions. *Journal of Geophysical Research*, VOL. 115, C01008, doi:10.1029/2009JC005433.
- Van der Westhuysen, A.J. (2010b). Improved Modelling of Wave-Current Interaction in SWAN. This volume.
- Van Vledder, G.Ph., M. Zijlema and L.H. Holthuijsen (2010). Revisiting the Jonswap Bottom Friction Formulation in Wind-Driven Storm Seas. This volume.
- Witteveen+Bos (2008). Hindcast of the 8 and 9 November 2007 storm for the tidal inlet of Ameland. Witteveen en Bos Report DT-293-2. Authors: R. Zijlstra and A. Smale.
- WL | Delft Hydraulics (2006a). SBW Plan of Action on the boundary conditions for the Waddenzee. WL | Delft Hydraulics Report H4750, April 2006.
- WL | Delft Hydraulics (2006b). Storm Hindcasts Norderneyer Seegat and Ameland Zeegat. WL | Delft Hydraulics Report H4803.11, August 2006.
- WL | Delft Hydraulics and Alkyon (2007). Sensitivity analysis of SWAN for the Ameland Zeegat. Report H4918.41. Authors: A. J. van der Westhuysen and G. Ph. van Vledder.
- Zijderveld, A. and H. Peters (2008). Measurement programme Dutch Wadden Sea. *Proceedings International Conference on Coastal Engineering*, pp. 404-410.
- Zijlema, M. (2009). Multiscale simulations using unstructured mesh SWAN model for wave hindcasting in the Dutch Wadden Sea. *Proceedings Coastal Dynamics*, Tokyo, Japan.

